TISSUE ENGINEERING: Part C
Volume 22, Number 10, 2016

DOI: 10.1089/ten.tec.2016.0257

termis
Tissue Engineering
& Regenerative Medicine
International Society

METHODS ARTICLE

Real-Time Force and Frequency Analysis of Engineered Human Heart Tissue Derived from Induced Pluripotent Stem Cells Using Magnetic Sensing

Kevin S. Bielawski, PhD,[1–3] Andrea Leonard, PhD,[1–3] Shiv Bhandari, MS,[2–4]
Chuck E. Murry, MD, PhD,[2–6] and Nathan J. Sniadecki, PhD[1–4]

Engineered heart tissues made from human pluripotent stem cell-derived cardiomyocytes have been used for modeling cardiac pathologies, screening new therapeutics, and providing replacement cardiac tissue. Current methods measure the functional performance of engineered heart tissue by their twitch force and beating frequency, typically obtained by optical measurements. In this article, we describe a novel method for assessing twitch force and beating frequency of engineered heart tissue using magnetic field sensing, which enables multiple tissues to be measured simultaneously. The tissues are formed as thin structures suspended between two silicone posts, where one post is rigid and another is flexible and contains an embedded magnet. When the tissue contracts it causes the flexible post to bend in proportion to its twitch force. We measured the bending of the post using giant magnetoresistive (GMR) sensors located underneath a 24-well plate containing the tissues. We validated the accuracy of the readings from the GMR sensors against optical measurements. We demonstrated the utility and sensitivity of our approach by testing the effects of three concentrations of isoproterenol and verapamil on twitch force and beating frequency in real-time, parallel experiments. This system should be scalable beyond the 24-well format, enabling greater automation in assessing the contractile function of cardiomyocytes in a tissue-engineered environment.

Introduction

Human induced pluripotent stem cell-derived cardiomyocytes (hiPSC-CMs) are used for developing cardiac therapies,[1–7] modeling cardiac development or disease,[7–11] and screening new drugs for efficacy or cardiotoxicity.[8,9,12,13] By studying hiPSC-CMs in engineered heart tissues, which are three-dimensional tissue constructs comprised of cardiomyocytes in a hydrogel, hiPSC-CMs show a more mature phenotype than two-dimensional cultured cardiomyocytes.[14–19] The three-dimensional environment recapitulates the cell–cell and cell–matrix interactions of the native myocardium, promoting hiPSC-CMs to have elongated shapes and a higher degree of myofibril organization. Since the primary role of cardiomyocytes *in vivo* is to forcibly contract to pump blood through the body, measuring twitch force and beating frequency is often relied upon as a functional assessment of hiPSC-CMs as it incorporates aspects of their electrical activity, calcium handing, and myofilament activation.

Several devices have been developed to grow engineered heart tissue and measure either beating frequency, or both beating frequency and twitch force.[20,21] Frequency-only systems include devices that measure beating rates of tissues in microfluidic channels[22] or devices that use microelectrode arrays.[23] There are also several devices that can measure twitch forces of tissue-like structures *in vitro*, including sheets of cells on flexible flaps,[24,25] sheets of cells on force transducers,[26] tissues on polyacrylamide gels,[27,28] and tissues suspended between load transducers[29,30] or polymeric posts.[31,32] Engineered heart tissues suspended between flexible, silicone posts enable one to detect the twitch forces generated by the tissues.[33,34] With silicone posts, some aspects of measuring twitch force and beating frequency can be automated.

[1]Department of Mechanical Engineering, University of Washington, Seattle, Washington.
[2]Center for Cardiovascular Biology, University of Washington, Seattle, Washington.
[3]Institute for Stem Cell and Regenerative Medicine, University of Washington, Seattle, Washington.
Departments of [4]Bioengineering, [5]Pathology and [6]Medicine/Cardiology, University of Washington, Seattle, Washington.

However, in our experience, they require dedicated microscopy equipment and custom image analysis routines to ensure accurate and consistent results.

In this article, we describe a novel tool for measuring the beating frequency and twitch force of myocardial tissues *in situ* through the use of magnetic field sensing. The system consists of engineered heart tissues suspended between silicone posts, where one post has an embedded magnet in its tip and the other is rigid from an embedded glass capillary tube (Fig. 1a). Tissue constructs on posts are placed into a 24-well tissue culture plate with giant magnetoresistive (GMR) sensors positioned below the plates. When a tissue construct beats, the force of its contraction cause the flexible post to deflect, thereby moving the position of the embedded magnet. The movement of the embedded magnet causes a voltage change at the GMR sensor, which in turn, is used to measure the force and frequency of the contractions.

Materials and Methods

Post fabrication

The posts were constructed using polydimethylsiloxane (PDMS, Sylgard 184; Dow Corning, Midland, MI) in a custom mold (Limited Productions, Inc., Bellevue, WA). First, a small amount of PDMS was poured into the mold and baked at 65°C to form the caps at the tips of the posts. After forming the caps, 1 mm^3 cubic magnets (MyMagnetMan, Largo, FL) were placed into sections of the mold that formed the flexible posts. Glass capillary tubes (1.1 mm diameter; Drummond Scientific Co., Broomall, PA) were placed into sections of the mold that formed the rigid posts. PDMS was then poured into the entire mold and cured overnight at 65°C. External magnets were used to hold the embedded magnets in place and maintain their orientation at the bottom of the posts while the PDMS cured. After the posts were removed from the mold, excess PDMS was trimmed away, yielding silicone posts that were 12.5 mm tall (including the 0.5 mm tall caps), 1.5 mm diameter, and spaced 8 mm apart (Fig. 1b, c).

Magnetic sensor array fabrication

GMR sensors (AAH002-02; NVE, Eden Prairie, MN) were arranged on printed circuit boards (OSH Park, Lake Oswego, OR) with other circuitry for filtering and amplifying the signal (Supplementary Fig. S1; Supplementary Data are available online at www.liebertpub.com/tec). The GMR sensors have a Wheatstone bridge configuration, so the voltage drop across the sensor changes with the magnetic field. Each measurement leg from the Wheatstone bridge was routed through high-pass filters using operational amplifiers (LM324; Texas Instruments, Dallas, TX). The signal was further amplified through the use of instrumentation amplifiers (INA118; Texas Instruments). Signals from the circuit board were routed to a data acquisition system (USB6002; National Instruments, Austin, TX). Custom software for voltage acquisition during biological experiments and both voltage and video acquisition during calibration experiments was made using LabView (National Instruments). The printed circuit boards with magnetic sensors

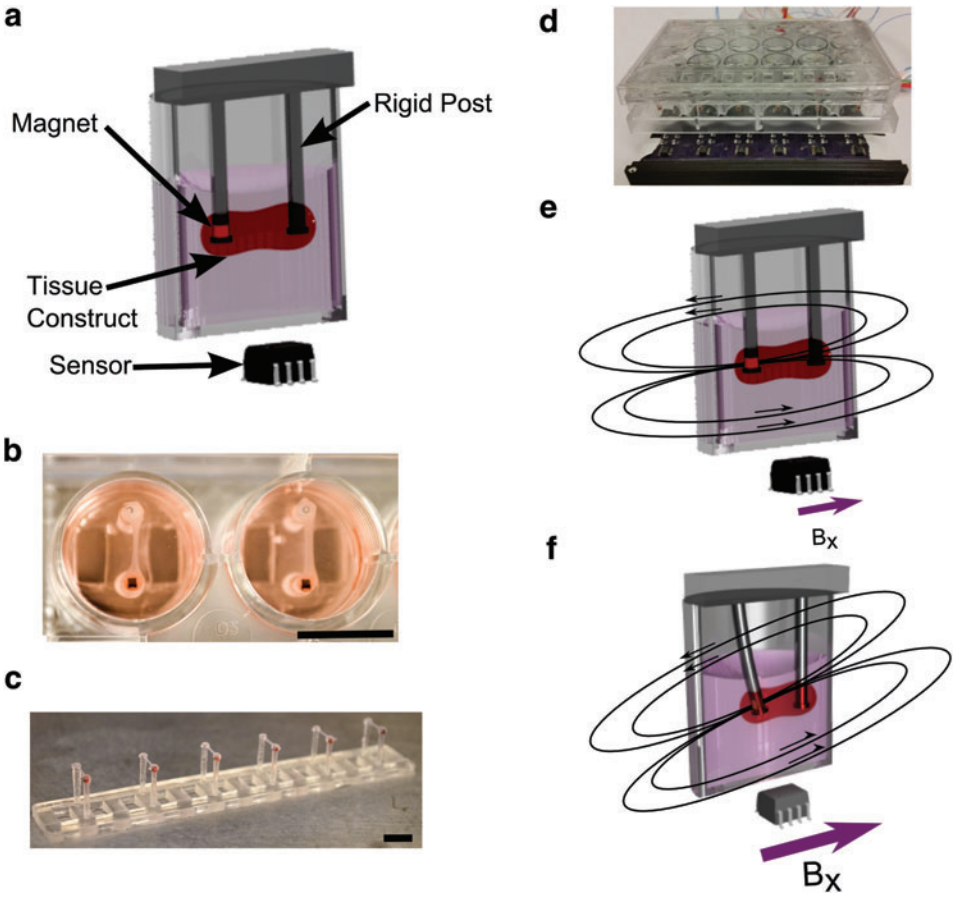

FIG. 1. Magnetic sensing used to determine twitch force and beating frequency in engineered heart tissue. **(a)** The approach consists of a tissue made from cardiomyocytes that is suspended between two silicone posts in a dish. A GMR sensor is located below the dish to detect the bending in the post with an embedded magnet. **(b)** Tissues fit into the wells of a 24-well plate. **(c)** Array of silicone posts with six tissues shown. **(d)** Layout of a set of six sensors arranged in parallel below a 24-well plate. The magnetic field changes in a linear fashion when the tissue moves from **(e)** diastole to **(f)** systole. Scale bars represent 10 mm. GMR, giant magnetoresistive. Color images available online at www.liebertpub.com/tec

were held in place using 3D-printed components and placed underneath a 24-well tissue culture plate (Fig. 1d). In this configuration, the array of sensors on the printed circuit board did not need to be sterilized and could be reused from experiment to experiment. A custom-molded lid for the 24-well plate was used to ensure that the array of posts in the 24-well plate was held in the proper position above the magnetic sensors. To make the lid, PDMS was poured into a mold, a lid of a 24-well dish was placed on top, and the assembly was cured overnight at 40°C. The result was a set of protrusions made from PDMS on the inside of the lid that secured the array of posts, keeping them at the correct position both laterally and longitudinally.

Magnetic model

A model of the system was developed in Matlab (Mathworks, Natick, MA) by treating the embedded magnet as a point dipole. A dipole approximation was used because the distance from the magnet to the sensor was much larger than the size of the magnet. The dipole of a magnet in a silicone post was determined experimentally to have a strength of $\mathbf{M} = 0.75\mathbf{e}_x + 0.15\mathbf{e}_y + 0.15\mathbf{e}_z$ [mA·m^2], where the origin of the coordinate system is at the magnet, $\mathbf{e}_x$ is the direction of the sensitive axis of the GMR sensor, $\mathbf{e}_y$ is its nonsensitive axis, and $\mathbf{e}_z$ is perpendicular to the plane containing $\mathbf{e}_x$ and $\mathbf{e}_y$. Since the GMR sensors measure the magnetic field in the sensitive direction and not in the other two directions, the x-component of the field produced by the embedded magnet was modeled as a projection onto the plane of the GMR sensor. The projection was determined based on the magnetic field of a point dipole,[35]

$$\vec{B} = \frac{\mu_0}{4\pi}\left[3\frac{(\vec{m}\cdot\vec{r})\,\vec{r}}{r^5} - \frac{\vec{m}}{r^3}\right],$$

where $\vec{B}$ is the magnetic flux density, μ_0 is the permeability of free space, $\vec{m}$ is the magnetic dipole moment, and $\vec{r}$ is the vector between the measurement point and the dipole. The vertical distance from the embedded magnet to the GMR sensor was determined to be 14 mm.

Device characterization

Devices were characterized by deflecting individual posts with a linear micro-positioner (SM-50; Newport Corp., Irvine, CA). The deflection of each post was viewed on an optical microscope (LV-100; Nikon, Tokyo, Japan) with a camera (OrcaFlash 2.8; Hamamatsu, Hamamatsu City, Japan). Images were recorded simultaneously with voltage readings from each GMR sensor using LabView software. Five different magnetic posts were used to characterize each sensor. The data were used to obtain a calibration constant for voltage-to-position measurements using linear-regression analysis with a least squares approach. The same configuration for characterization was used for all subsequent experiments with engineered heart tissue.

Engineered heart tissue generation

Undifferentiated human induced pluripotent stem cells (hiPSCs) from the IMR90 line, were maintained in mTeSR (Stemcell Technologies, Vancouver, Canada) on tissue culture dishes coated with Matrigel (Corning, Corning, NY). An established protocol for directed differentiation was used to derive cardiomyocytes (CMs), as previously described.[36] Differentiation yielded greater than 80% cardiomyocytes that were positive for cardiac troponin T by flow cytometry. hiPSC-CMs were cast into engineered heart tissue on day 24 after induction of differentiation. Tissue constructs were generated following a similar protocol to Schaaf *et al.*,[37] where each tissue was cast from a 100 μL fibrin gel solution containing 5×10^5 hiPSC-CMs and 5×10^4 supporting stromal cells (line HS-27a[38]). Agarose wells were formed by pouring a 2% agarose solution into a 24-well plate fitted with custom built spacers. A pair of posts was positioned into each agarose well, and the cell-laden gel solution was poured into the well to create a tissue construct bound onto the tips of each post. After 80 min of time for gelation, the newly formed tissues were transferred to a fresh 24-well plate. Engineered heart tissues were maintained in a 24-well plate and were supplied with fresh RPMI media (11875-119; Invitrogen, Carlsbad, CA), supplemented with B-27 plus insulin (17504044; Life Technologies, Carlsbad, CA), and 5 mg/mL aminocaproic acid (A2504; Sigma-Aldrich, St. Louis, MO), three times per week. The tissue constructs were maintained in culture for 2 weeks before testing, for sufficient compaction and development of a stable beating pattern. From our observations, tissues achieve a maximal force after 2–3 weeks in culture. We did not observe any muscle fatigue in the tissues during the course of our experiments.

Frequency and force plotting

Voltage outputs from the magnetic sensors were recorded using LabView and displayed on a screen for real-time monitoring during experiments. Further analysis was performed on all experiments to assess the frequency and magnitude of contractions over time. The data were filtered with a low-pass filter to remove measurement noise using an eighth order Butterworth filter with a cutoff frequency of 7 Hz. Only the peak-to-peak amplitudes were analyzed for force measurements, so low-frequency fluctuations in baseline readings were eliminated from the signal. To eliminate low-frequency baseline drifts, an exponential moving average filter with an exponent constant of 0.0001 was used.

After filtering the data, custom-written code in Matlab for peak finding was used to identify the maxima and minima of the data to calculate twitch force and beating frequency. Twitch force was determined by subtracting the voltage at a maximum from an adjacent minimum, as long as the maximum and minimum were within 2 s of each other, and then converting from voltage to force based upon the calibration of the GMR sensor and the bending stiffness of the silicone posts. Beating frequency was determined based on the time between maxima.

A cutoff reading of 7 mV was chosen based on analysis of the signal produced by nonbeating tissues. Below this threshold, there was an increased chance of registering a false beat due to noise in the system. Furthermore, during drug testing, a tissue was determined to have stopped beating when the frequency of beats fell below 0.2 Hz. To reduce errors due to a disturbance in the posts during the addition of reagents, a 4-s window of time was removed from the averages for both twitch force and beating frequency. A combined 10-s moving average of the twitch force and beating frequency was obtained for each of the four experiments.

Pacing experiments

To compare the waveforms of tissues measured magnetically to tissues measured optically, tissues were paced at 1.5 and 2 Hz in both platforms. Both measurements were taken with the tissues and sensors at 37°C. Carbon rods were used as electrodes and affixed with PDMS to the bottom of 24-well plate dishes. Platinum wire was wrapped around the electrodes, and connected to a stimulator (S88X; Astro-Med, Inc., West Warwick, RI). Biphasic pacing was used with a pulse duration of 5 ms and pulse amplitude of 5 V for both conditions. The tissues were observed to follow the electrical stimulation and produced twitch forces with consistent amplitude during pacing. Optical measurements were taken with an inverted microscope (Eclipse Ti; Nikon, Inc., Melville, NY) using a CCD camera (Clara, Andor, Belfast, Northern Ireland). The position of the flexible post as a function of time was determined using custom-written code for image analysis developed in Matlab. Determination of the location of the post using magnetic sensing was performed using the methods described above.

Pharmacological testing

Experiments were performed using verapamil hydrochloride (CAS 152-11-4; Tocris Bioscience, Bristol, United Kingdom) and isoproterenol hydrochloride (CAS 5984-95-2; Sigma-Aldrich, St. Louis, MO). Verapamil is a calcium channel blocker,[39] while isoproterenol is a β-adrenergic agonist,[40] and both alter twitch force and beating frequency in the adult heart. All tissues were treated with 50 μL of a mixture of the relevant drug in DI water. A batch mixture of 2.5 mM of each drug in DI water was passed through a sterile filter and portioned into the appropriate dilution based on the final concentration. The media volume in each well during the experiment was 2.5 mL, and 50 mL of the drug solution was added to yield the desired final concentration of the drug in the complete media. The control case had no treatment added to the media during the experiment. The sham control had 50 μL of DI water added to the media. All experiments with drugs were performed at 37°C. Drugs were washed out with new media and tissues were allowed to reset for 2 days before undergoing further treatments. The twitch force and frequency was measured for four tissues per condition.

Results

Engineered heart tissue fabricated onto magnetic post arrays

The twitch forces and beating frequency of engineered heart tissue have been measured previously using pairs of silicone posts, where both posts deflect when a tissue undergoes a twitch contraction.[33,34] Here, we built a similar array of posts, but where one post was flexible and magnetic, while the other was rigid and nonmagnetic. When a tissue contracts, it causes a deflection in the magnetic post with negligible deflection in the rigid post (Fig. 1e, f). The deflection of the magnetic post changes the magnetic field at the GMR sensor, which reports the change as voltage signal. Posts were made out of polydimethylsiloxane (PDMS) and were evenly spaced as an array for insertion into a 24-well plate (Fig. 1b, c). Caps on each post were used to prevent the detachment of the tissues during culture. Based upon the dimensions of the posts and its behavior as a cantilever, there is a linear relationship between the deflection of the post and the force of the tissue. The dimensions of the post, along with a Young's modulus of 2.5 MPa for PDMS, resulted in a bending stiffness of 0.98 μN/μm, calculated by assuming the net tissue force acts at the tip of the post, and using the method described by Schoen *et al.*[41] Thus, we developed an approach where twitch force of an engineered heart tissue causes its magnetic post to deflect linearly, which can be detected by the reading of the GMR sensor underneath the culture dish.

Magnetic sensing of post deflections

GMR sensors were soldered to printed circuit boards containing circuitry for high-pass filters and instrumentation amplifiers. After signal conditioning, the voltage reading from the GMR sensors were passed to a data acquisition system running custom software to record the deflections of the magnetic posts. In addition to recording the data, it was possible to monitor the deflection in real-time.

The location with the highest measurement sensitivity for the GMR sensors was determined by modeling of the magnetic field produced by the neodymium magnet. Specifically, we analyzed the change in the magnetic field due to a 300 μm deflection in a magnetic post (Fig. 2a), which is on the larger end of observed post deflections. Our results indicated that in a layout for a 24-well culture plate, there is minimal crosstalk between the magnetic post and its neighboring sensors in adjacent wells, for this 300 μm deflection. In addition, the optimal location for the GMR sensor in the plane 14 mm below the TC dish could be determined with this model, which was approximately a 3.5 mm offset from the point directly below the magnetic post (Fig. 2b). This offset location was due to the translation and rotation of the magnetic dipole during the post motion. The model further predicts a linear response for displacements up to 2 mm, which indicates that the upper limit in a reading is 1.96 mN (Supplementary Fig. S2). Based upon a cutoff reading of 7 mV, the lower limit is 26 μN. Thus, these results demonstrate that there is an ideal location for the magnetic sensor and that there is little interference in detecting the beating frequencies and twitch forces in tissues that neighbor each other in a 24-well plate.

Characterization of magnetic sensing

A custom manipulator system was built to move the posts manually while tracking the position and measuring the voltage changes. Due to a 0.16 Hz cutoff frequency on the high-pass filters integrated into the circuit design, dynamic motion of the posts was required to properly calibrate the system. We calibrated the relationship between the motion of the posts and the voltage output by placing the arrays under a reflective microscope. Posts were dynamically moved using a linear micro-positioner while simultaneously monitoring the voltage outputs.

Five different arrays of magnetic posts were used to calibrate the system (Supplementary Fig. S3). The trend for each sensor was quite linear (R^2 >0.90) and produced a signal within the expected range based on the models and the expected motions of the posts with engineered heart tissue (Fig. 2c). Each sensor had a different calibration coefficient, likely due to variability in the sensor fabrication, circuitry, and layout of the sensors on the device. Although

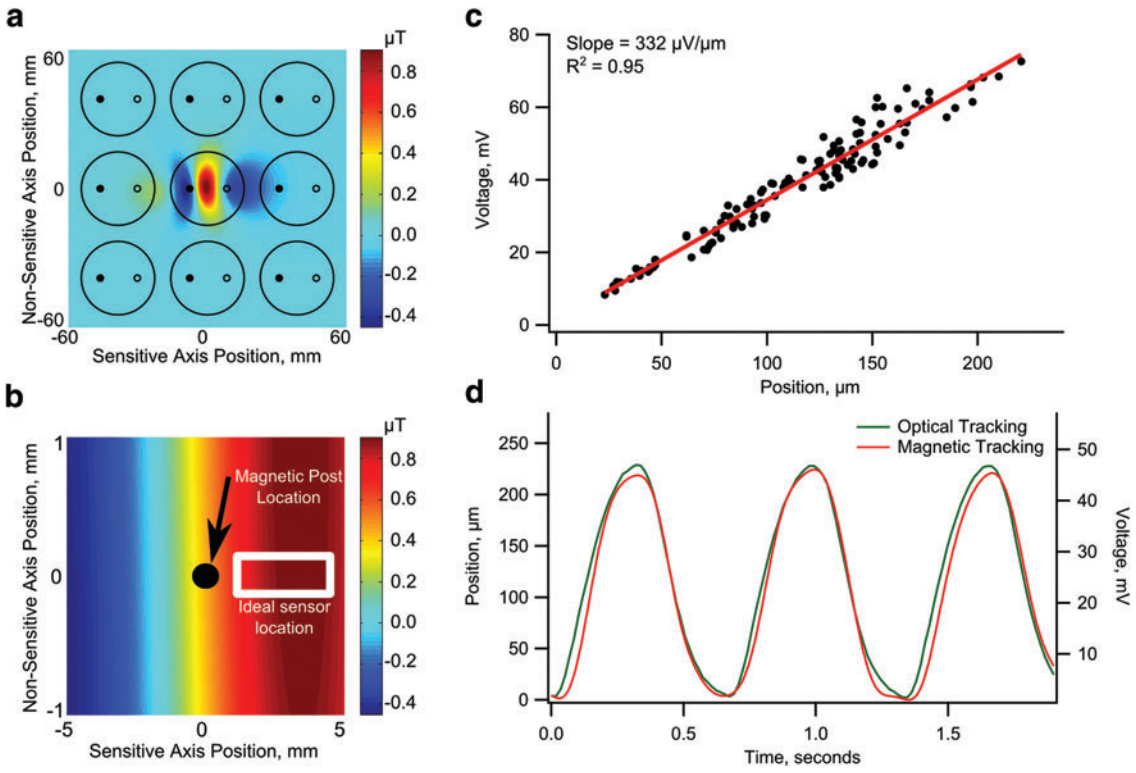

FIG. 2. Calibration of magnetic sensing. **(a)** Magnetic fields are not expected to affect readings on other posts. **(b)** Optimal placement of a magnetic sensor is ~3.5 mm ahead of the magnetic post in the direction in which it bends. **(c)** Each sensor has a linear voltage-position reading for the ranges of expected engineered heart tissue forces. **(d)** There is a strong correlation between position measured optically and the position calculated by the calibrated magnetic sensors. Color images available online at www.liebertpub.com/tec

the sensors did have minor variations, the trend for each individual sensor was linear. Hence, this characterization showed that we can model the force of each tissue by directly relating the voltage change to post deflection.

Comparing optical and magnetic readings of engineered heart tissue

Engineered heart tissues containing hiPSC-CMs and stromal cells spanned between the magnetic and rigid PDMS post pairs within 24-well tissue culture dishes. After 2 weeks of culture, the tissue constructs were beating with uniform and stable contractions, which deflected the tip of the flexible posts between 100 and 300 μm during each twitch. Each tissue construct showed consistent force production when electrically paced. Within a 10-min window, the contractions of a tissue construct were recorded under optical microscopy and then transferred to the GMR sensors for magnetic tracking. A strong correlation of the waveform for the deflection of the post was observed between optical tracking and magnetic tracking (Fig. 2d). This result demonstrated that the magnetic system is suitable for measuring the beating frequency and twitch force as optical tracking.

Pharmacological testing

One of the benefits of this device is the ability to simultaneously study the effects of drugs on the twitch force and beating frequency of tissues in real time. The ability for parallel studies was demonstrated using three concentrations of both isoproterenol and verapamil. Isoproterenol, a β-adrenergic agonist, and verapamil, a calcium channel blocker, were chosen for their well-studied effects on cardiomyocytes. In general, verapamil lowers twitch forces,[42] while isoproterenol increases beating frequency and, for adult cardiomyocytes, beating force.[40] All of the tissues were measured on the magnetic sensors for 1 min before adding drugs to the system. Twitch force and beating frequency of the tissues was monitored for at least 3 min after the addition of drug or vehicle. We noted that there was variation in the baseline twitch force and beating frequency between tissues before the addition of drugs.

In order to compare the effects of the drugs, relative twitch force and beating frequency was used to determine the percent change of each tissue over time. Each study generated complete waveforms of the twitch contractions over the course of at least 3 min (Fig. 3). A set of tissues were not given any drug as a control or given water as a sham control. In both cases, the spontaneous beating of the tissues had little variation throughout the experiments.

Verapamil had a large effect on both the beating frequency and the force generation of the tissue constructs (Fig. 4). Increasing concentrations of verapamil caused lower forces and lower frequencies. The effect of verapamil on force was nearly immediate, although there typically was an initial increase in beating frequency before it was reduced. A low dosage of verapamil caused a slight increase of the beating frequency from the baseline frequency. There were some fairly large variations in the verapamil beating frequency and force magnitude, some of which can be

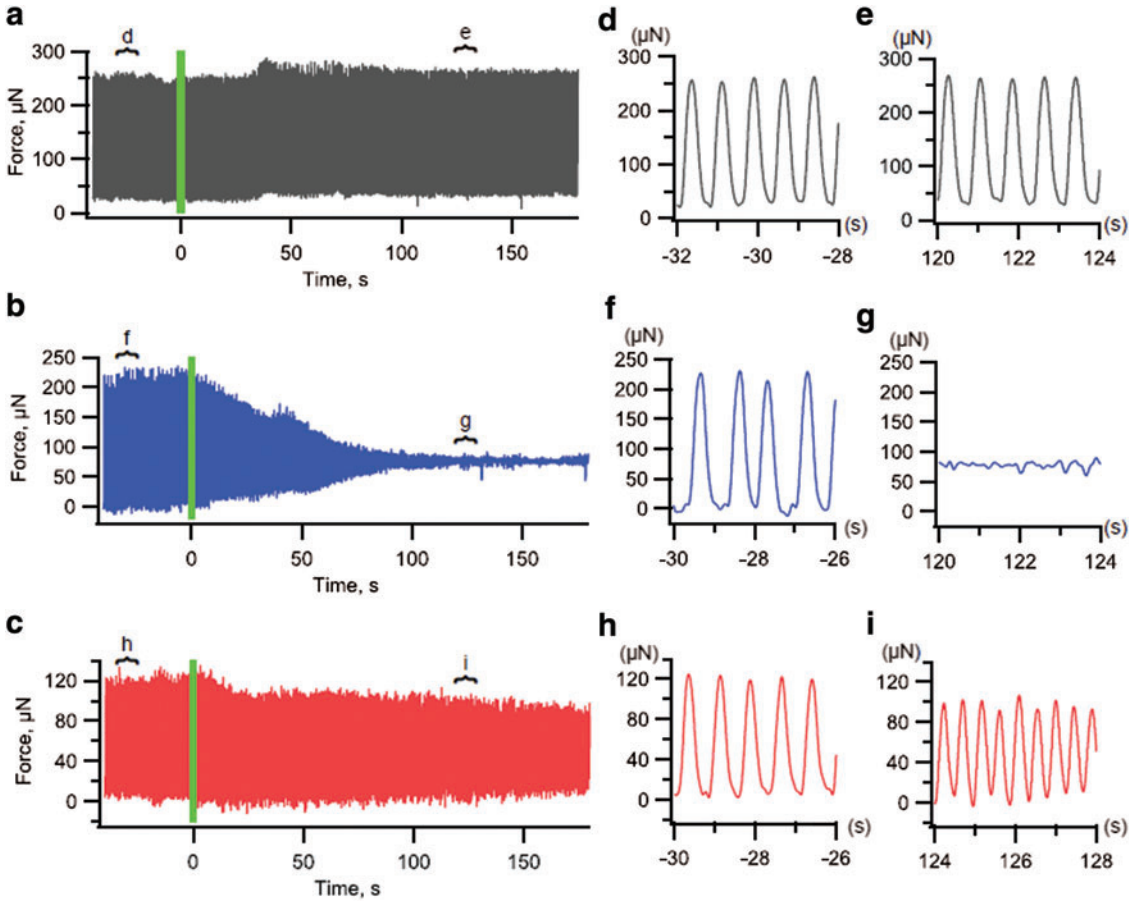

FIG. 3. Real-time analysis of tissue forces (representative force-time profiles) in response to pharmacological compounds. **(a)** Sham control has a similar force and frequency profile over time. Tissues treated with **(b)** 5 μM of verapamil have a significantly reduced force over time, while tissues treated with **(c)** 500 nM of isoproterenol have a reduced force and significantly increased frequency over time. **(d, f,** and **h)** Tissues have similar frequencies and twitch force magnitudes before adding pharmacological compounds. **(e)** Sham control continues at the same force and frequency, while tissues treated with **(g)** verapamil eventually stop beating, and tissues treated with **(i)** isoproterenol have nearly double the beating frequency and a slightly reduced force. Color images available online at www.liebertpub.com/tec

attributed to the choice of a 7 mV cutoff for force generation. This was due to the amount of noise in the system.

As expected, isoproterenol increased the beating frequency as the concentration was increased. The increase in beating frequency started quickly, and appeared to level off within 2 min after adding the drug, (Fig. 4). A decrease in contractile force was observed with increasing concentrations of isoproterenol. The decrease in force is typical for immature myocardium, which has not yet expressed phospholamban, the Ca^{2+}-regulatory protein that is targeted by beta-adrenergic stimulation.[33,43,44] These results indicated that our system is sensitive to changes in twitch force and frequency to measure the effects of drugs and could be used in a drug screening assay.

Discussion

In this article we have developed a novel platform for real-time magnetic measurements of twitch forces and beating frequencies of engineered heart tissues derived from hiPSC-CMs. We designed our system so that the tissue constructs spanned between a pair of silicone posts, where one was rigid and another was flexible and contains an embedded magnet. The motion of the magnet was tracked using a GMR sensor located underneath a 24-well plate to determine the force of the tissue. We characterized the system against optical tracking of the post deflection and showed a linear response of voltage to tissue force. Finally, we used different concentrations of isoproterenol and verapamil to demonstrate the utility of the device to measure twitch force and frequency in real-time parallel experiments.

Several tools have been developed for monitoring the beating frequency and twitch force production of EHTs, but thus far, none have produced simple measurements to enable real-time contractile information. Previous devices have looked into electrical measurements of force using PDMS devices,[45] and other devices have embedded magnetic material into PDMS cantilever devices.[46,47] Few devices have used magnetic field changes to measure forces,[48] and we believe that this is the first device to measure tissue forces using embedded magnets in a PDMS device. The device provides some key advantages as it is able to continuously monitor the forces of several tissue constructs throughout an experiment. Real-time monitoring can ensure that tissues are behaving properly and it can aid in performing massively parallel experiments. In this article, the system was limited to six simultaneous measurements, but, as shown in Figure 2a, the system could be expanded to

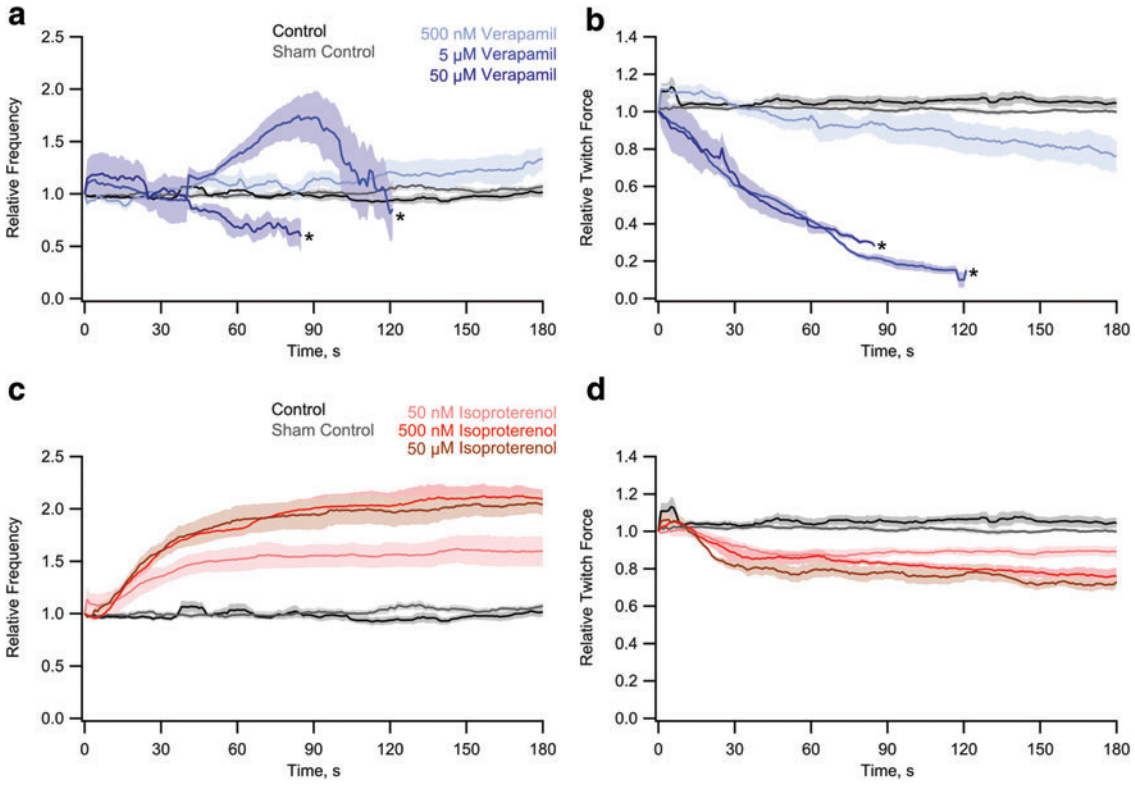

FIG. 4. Combined data from multiple experiments with verapamil and isoproterenol. **(a)** Frequency of contractions increases with verapamil addition while **(b)** magnitude of twitch forces decreases (asterisks indicate when the signal for more than half of the data tested fell below 7 mV and 0.2 Hz). Isoproterenol increases the **(c)** frequency of tissue contractions, and slightly lowers the **(d)** twitch forces of tissue contractions. Shaded regions represent standard error of four tissues per group. Color images available online at www.liebertpub.com/tec

simultaneously monitor an entire 24-well plate. Even with only six simultaneous measurements, four arrays of posts were tested with two controls and four measurements in rapid succession without the need to position the posts or find the posts in a microscope objective. This rapid screening can be useful for high-throughput, low-cost monitoring of engineered heart tissues for drug screening or tissue replacement applications.

To demonstrate the utility of this device, two different drugs were used to alter the frequency and force of tissue contractions. Verapamil was chosen as a calcium channel blocker to reduce contractile force and frequency while isoproterenol was chosen as a β-adrenergic agonist with the expected effect of increasing contraction frequency. We found verapamil to lower both contractile force and frequency, and temporarily stop the tissue construct from beating. Furthermore, we found that the frequency of contractions increased before the contractions ceased to beat with detectable forces for higher concentrations of verapamil. For a low concentration of verapamil, we found that the frequency increased, while the magnitude of forces had a slight decrease. The increased frequency and lowered force response of EHTs to verapamil has been seen before,[49–51] and is now able to be measured *in situ* and in real time.

Isoproterenol increased the frequency along the same order as what had been seen previously.[27,52] The response was a steady over the course of ~90 s. After 90 s, the response leveled off to the new frequency and twitch force. Somewhat surprisingly, the force of contractions decreased, however, it has been shown that EHTs derived from induced pluripotent stem cells have different responses than that of native heart tissues.[53] The structure of induced pluripotent stem cells used in these experiments is likely much more immature than adult cardiomyocytes,[44] and it has been shown that immature cardiomyocyte tissues do not produce as strong a force response to isoproterenol.[43]

This system was used to simultaneously measure the response of six different tissues at a time, and four replicates were easily measured in the time it took the tissues to respond to the forces. Little adjustment or calibration was necessary once the device was built, and postprocessing analysis could easily be integrated into the data acquisition program to produce immediate results from experiments using this system. Furthermore, the tissue constructs and multi-well dishes are all disposable, while the sensors and electronics are free from contacting the biological media, and thus do not require sterilization between each use. This enables testing of devices over time for studies that have slower-acting drugs, or to monitor the twitch forces of tissues in an incubator over time. This system can be used to either rapidly screen for a number of different drugs or to monitor the contractile forces of EHTs being developed for potential therapeutic replacements.

To expand the utility of the device for rapid and simultaneous measurements of twitch force and frequency, some aspects of the device presented here would need improvement. Currently, this system is able to measure twitch forces, but is not able to measure passive tension, that is, when the tissue is in diastole, due to the high-pass filter. The system could alter the filtering design to measure passive

tension of the tissues. In addition, placement of sensors could be further improved to reduce variance between each sensor. These improvements can be engineered to provide more information about cardiomyocytes and provide an inexpensive and autonomous platform for functional assessment of hiPSC-CMs or other cardiomyocytes.

Acknowledgments

The authors wish to acknowledge support from the National Science Foundation (CBET-1509105, CMMI-1402673 to N.J.S.), the National Institutes of Health (F32 HL126332 to A.L.; R01 HL084642, P01 HL094374, P01 GM81619, U01 HL100405 to C.E.M.), and the Fondation Leducq Transatlantic Network of Excellence (to C.E.M.).

Disclosure Statement

K.S.B. has equity in Stasys Medical Corporation. C.E.M. is a cofounder and has equity in BEAT Biotherapeutics. N.J.S. is a cofounder and has equity in Stasys Medical Corporation.

References

1. Karantalis, V., Balkan, W., Schulman, I.H., Hatzistergos, K.E., and Hare, J.M. Cell-based therapy for prevention and reversal of myocardial remodeling. Am J Physiol Heart Circ Physiol **303,** 2012.
2. Suncion, V.Y., Schulman, I.H., and Hare, J.M. Concise review: the role of clinical trials in deciphering mechanisms of action of cardiac cell-based therapy. Stem Cells Transl Med **1,** 2012.
3. Kawamura, M., Miyagawa, S., Miki, K., Saito, A., Fukushima, S., Higuchi, T., Kawamura, T., Kuratani, T., Daimon, T., Shimizu, T., Okano, T., and Sawa, Y. Feasibility, safety, and therapeutic efficacy of human induced pluripotent stem cell-derived cardiomyocyte sheets in a porcine ischemic cardiomyopathy model. Circulation **126,** 2012.
4. Mauritz, C., Martens, A., Rojas, S.V., Schnick, T., Rathert, C., Schecker, N., Menke, S., Glage, S., Zweigerdt, R., Haverich, A., Martin, U., and Kutschka, I. Induced pluripotent stem cell (ipsc)-derived flk-1 progenitor cells engraft, differentiate, and improve heart function in a mouse model of acute myocardial infarction. Eur Heart J **32,** 2011.
5. Singla, D.K., Long, X., Glass, C., Singla, R.D., and Yan, B. Induced pluripotent stem (ips) cells repair and regenerate infarcted myocardium. Mol Pharm **8,** 2011.
6. Mosna, F., Annunziato, F., Pizzolo, G., and Krampera, M. Cell therapy for cardiac regeneration after myocardial infarct: which cell is the best? Cardiovasc Hematol Agents Med Chem **8,** 2010.
7. Freund, C., and Mummery, C.L. Prospects for pluripotent stem cell-derived cardiomyocytes in cardiac cell therapy and as disease models. J Cell Biochem **107,** 2009.
8. Bellin, M., Marchetto, M.C., Gage, F.H., and Mummery, C.L. Induced pluripotent stem cells: the new patient? Nat Rev Mol Cell Biol **13,** 2012.
9. Grskovic, M., Javaherian, A., Strulovici, B., and Daley, G.Q. Induced pluripotent stem cells—opportunities for disease modelling and drug discovery. Nat Rev Drug Discov **10,** 2011.
10. Dambrot, C., Passier, R., Atsma, D., and Mummery, C.L. Cardiomyocyte differentiation of pluripotent stem cells and their use as cardiac disease models. Biochem J **434,** 2011.
11. Das, A.K., and Pal, R. Induced pluripotent stem cells (ipscs): the emergence of a new champion in stem cell technology-driven biomedical applications. J Tissue Eng Regen Med **4,** 2010.
12. Mercola, M., Colas, A., and Willems, E. Induced pluripotent stem cells in cardiovascular drug discovery. Circ Res **112,** 2013.
13. Tzatzalos, E., Abilez, O.J., Shukla, P., and Wu, J.C. Engineered heart tissues and induced pluripotent stem cells: macro- and microstructures for disease modeling, drug screening, and translational studies. Adv Drug Deliv Rev **96,** 2016.
14. Eder, A., Vollert, I., Hansen, A., and Eschenhagen, T. Human engineered heart tissue as a model system for drug testing. Adv Drug Deliv Rev **96,** 214, 2016.
15. Zimmermann, W.-H., Melnychenko, I., and Eschenhagen, T. Engineered heart tissue for regeneration of diseased hearts. Biomaterials **25,** 1639, 2004.
16. Hirt, M.N., Hansen, A., and Eschenhagen, T. Cardiac tissue engineering: state of the art. Circ Res **114,** 354, 2014.
17. Tiburcy, M., and Zimmermann, W.-H. Modeling myocardial growth and hypertrophy in engineered heart muscle. Trends Cardiovasc Med **24,** 7, 2014.
18. Iyer, R.K., Chiu, L.L., Reis, L.A., and Radisic, M. Engineered cardiac tissues. Curr Opin Biotechnol **22,** 706, 2011.
19. Turnbull, I.C., Karakikes, I., Serrao, G.W., Backeris, P., Lee, J.-J., Xie, C., Senyei, G., Gordon, R.E., Li, R.A., and Akar, F.G. Advancing functional engineered cardiac tissues toward a preclinical model of human myocardium. FASEB J **28,** 644, 2014.
20. Zimmermann, W.-H., Didié, M., Wasmeier, G.H., Nixdorff, U., Hess, A., Melnychenko, I., Boy, O., Neuhuber, W.L., Weyand, M., and Eschenhagen, T. Cardiac grafting of engineered heart tissue in syngenic rats. Circulation **106,** I-151, 2002.
21. Mannhardt, I., Breckwoldt, K., Letuffe-Breniere, D., Schaaf, S., Schulz, H., Neuber, C., Benzin, A., Werner, T., Eder, A., Schulze, T., Klampe, B., Christ, T., Hirt, M.N., Huebner, N., Moretti, A., Eschenhagen, T., and Hansen, A. Human engineered heart tissue: analysis of contractile force. Stem cell reports 2016.
22. Mathur, A., Loskill, P., Shao, K., Huebsch, N., Hong, S., Marcus, S.G., Marks, N., Mandegar, M., Conklin, B.R., and Lee, L.P. Human ipsc-based cardiac microphysiological system for drug screening applications. Sci Rep **5,** 8883, 2015.
23. Navarrete, E.G., Liang, P., Lan, F., Sanchez-Freire, V., Simmons, C., Gong, T., Sharma, A., Burridge, P.W., Patlolla, B., and Lee, A.S. Screening drug-induced arrhythmia using human induced pluripotent stem cell-derived cardiomyocytes and low-impedance microelectrode arrays. Circulation **128,** S3, 2013.
24. Grosberg, A., Alford, P.W., McCain, M.L., and Parker, K.K. Ensembles of engineered cardiac tissues for physiological and pharmacological study: heart on a chip. Lab Chip **11,** 2011.
25. Agarwal, A., Goss, J.A., Cho, A., McCain, M.L., and Parker, K.K. Microfluidic heart on a chip for higher throughput pharmacological studies. Lab Chip **13,** 3599, 2013.
26. Zhang, D., Shadrin, I.Y., Lam, J., Xian, H.-Q., Snodgrass, H.R., and Bursac, N. Tissue-engineered cardiac patch for advanced functional maturation of human esc-derived cardiomyocytes. Biomaterials **34,** 5813, 2013.
27. Hayakawa, T., Kunihiro, T., Ando, T., Kobayashi, S., Matsui, E., Yada, H., Kanda, Y., Kurokawa, J., and Furukawa, T.

Image-based evaluation of contraction–relaxation kinetics of human-induced pluripotent stem cell-derived cardiomyocytes: correlation and complementarity with extracellular electrophysiology. J Mol Cell Cardiol **77,** 178, 2014.
28. Aung, A., Bhullar, I.S., Theprungsirikul, J., Davey, S.K., Lim, H.L., Chiu, Y.-J., Ma, X., Dewan, S., Lo, Y.-H., and McCulloch, A. 3d cardiac μtissues within a microfluidic device with real-time contractile stress readout. Lab on a Chip **16,** 153, 2016.
29. Tulloch, N.L., Muskheli, V., Razumova, M.V., Korte, F.S., Regnier, M., Hauch, K.D., Pabon, L., Reinecke, H., and Murry, C.E. Growth of engineered human myocardium with mechanical loading and vascular coculture. Circ Res **109,** 47, 2011.
30. Ruan, J.L., Tulloch, N.L., Saiget, M., Paige, S.L., Razumova, M.V., Regnier, M., Tung, K.C., Keller, G., Pabon, L., and Reinecke, H. Mechanical stress promotes maturation of human myocardium from pluripotent stem cell-derived progenitors. Stem Cells **33,** 2148, 2015.
31. Eschenhagen, T., Fink, C., Remmers, U., Scholz, H., Wattchow, J., Weil, J., Zimmermann, W., Dohmen, H., Schäfer, H., and Bishopric, N. Three-dimensional reconstitution of embryonic cardiomyocytes in a collagen matrix: a new heart muscle model system. FASEB J **11,** 683, 1997.
32. Boudou, T., Legant, W.R., Mu, A., Borochin, M.A., Thavandiran, N., Radisic, M., Zandstra, P.W., Epstein, J.A., Margulies, K.B., and Chen, C.S. A microfabricated platform to measure and manipulate the mechanics of engineered cardiac microtissues. Tissue Eng Part A **18,** 910, 2011.
33. Schaaf, S., Shibamiya, A., Mewe, M., Eder, A., Stöhr, A., Hirt, M.N., Rau, T., Zimmermann, W.-H., Conradi, L., and Eschenhagen, T. Human engineered heart tissue as a versatile tool in basic research and preclinical toxicology. PLoS One **6,** e26397, 2011.
34. Stoehr, A., Neuber, C., Baldauf, C., Vollert, I., Friedrich, F.W., Flenner, F., Carrier, L., Eder, A., Schaaf, S., and Hirt, M.N. Automated analysis of contractile force and ca2+ transients in engineered heart tissue. Am J Physiol Heart Circ Physiol **306,** H1353, 2014.
35. Coey, J.M., Magnetism and Magnetic Materials. New York, NY: Cambridge University Press, 2010.
36. Laflamme, M.A., Chen, K.Y., Naumova, A.V., Muskheli, V., Fugate, J.A., Dupras, S.K., Reinecke, H., Xu, C., Hassanipour, M., and Police, S. Cardiomyocytes derived from human embryonic stem cells in pro-survival factors enhance function of infarcted rat hearts. Nat Biotechnol **25,** 1015, 2007.
37. Schaaf, S., Eder, A., Vollert, I., Stöhr, A., Hansen, A., and Eschenhagen, T. Generation of strip-format fibrin-based engineered heart tissue (EHT). Methods Mol Biol **1181,** 121, 2014.
38. Roecklein, B.A., and Torok-Storb, B. Functionally distinct human marrow stromal cell lines immortalized by transduction with the human papilloma virus e6/e7 genes. Blood **85,** 997, 1995.
39. Sperelakis, N. Electrophysiology of calcium antagonists. J Mol Cell Cardiol **19,** 19, 1987.
40. Endoh, M. The effects of various drugs on the myocardial inotropic response. Gen Pharmacol **26,** 1, 1995.
41. Schoen, I., Hu, W., Klotzsch, E., and Vogel, V. Probing cellular traction forces by micropillar arrays: contribution of substrate warping to pillar deflection. Nano Lett **10,** 1823, 2010.
42. Schwinger, R.H., Böhm, M., and Erdmann, E. Negative inotropic properties of isradipine, nifedipine, diltiazem, and verapamil in diseased human myocardial tissue. J Cardiovasc Pharmacol **15,** 892, 1990.
43. Pillekamp, F., Haustein, M., Khalil, M., Emmelheinz, M., Nazzal, R., Adelmann, R., Nguemo, F., Rubenchyk, O., Pfannkuche, K., and Matzkies, M. Contractile properties of early human embryonic stem cell-derived cardiomyocytes: beta-adrenergic stimulation induces positive chronotropy and lusitropy but not inotropy. Stem Cells Dev **21,** 2111, 2012.
44. Yang, X., Pabon, L., and Murry, C.E. Engineering adolescence maturation of human pluripotent stem cell–derived cardiomyocytes. Circ Res **114,** 511, 2014.
45. Noda, K., Hoshino, K., Matsumoto, K., and Shimoyama, I. A shear stress sensor for tactile sensing with the piezoresistive cantilever standing in elastic material. Sensor Actuat A-Phys **127,** 295, 2006.
46. Evans, B., Shields, A., Carroll, R.L., Washburn, S., Falvo, M., and Superfine, R. Magnetically actuated nanorod arrays as biomimetic cilia. Nano Lett **7,** 1428, 2007.
47. Sniadecki, N.J., Anguelouch, A., Yang, M.T., Lamb, C.M., Liu, Z., Kirschner, S.B., Liu, Y., Reich, D.H., and Chen, C.S. Magnetic microposts as an approach to apply forces to living cells. Proc Natl Acad Sci **104,** 14553, 2007.
48. Hein, M.A., Maqableh, M.M., Delahunt, M.J., Tondra, M., Flatau, A.B., Shield, C.K., and Stadler, B.J. Fabrication of bioinspired inorganic nanocilia sensors. IEEE Trans Magn **49,** 191, 2013.
49. Mehta, A., Chung, Y.Y., Ng, A., Iskandar, F., Atan, S., Wei, H., Dusting, G., Sun, W., Wong, P., and Shim, W. Pharmacological response of human cardiomyocytes derived from virus-free induced pluripotent stem cells. Cardiovasc Res **91,** 577, 2011.
50. Himmel, H.M. Drug-induced functional cardiotoxicity screening in stem cell-derived human and mouse cardiomyocytes: effects of reference compounds. J Pharmacol Toxicol Methods **68,** 97, 2013.
51. Gilchrist, K.H., Lewis, G.F., Gay, E.A., Sellgren, K.L., and Grego, S. High-throughput cardiac safety evaluation and multi-parameter arrhythmia profiling of cardiomyocytes using microelectrode arrays. Toxicol Appl Pharmacol **288,** 249, 2015.
52. Kim, J.J., Yang, L., Lin, B., Zhu, X., Sun, B., Kaplan, A.D., Bett, G.C., Rasmusson, R.L., London, B., and Salama, G. Mechanism of automaticity in cardiomyocytes derived from human induced pluripotent stem cells. J Mol Cell Cardiol **81,** 81, 2015.
53. Xi, J., Khalil, M., Shishechian, N., Hannes, T., Pfannkuche, K., Liang, H., Fatima, A., Haustein, M., Suhr, F., and Bloch, W. Comparison of contractile behavior of native murine ventricular tissue and cardiomyocytes derived from embryonic or induced pluripotent stem cells. FASEB J **24**, 2739, 2010.

Address correspondence to:
Nathan J. Sniadecki, PhD
Department of Mechanical Engineering
University of Washington
Campus Box 352600
Seattle, WA 98195

E-mail: nsniadec@uw.edu

Received: June 29, 2016
Accepted: September 6, 2016
Online Publication Date: September 28, 2016